Convolutional Neural Networks for Prostate Magnetic Resonance Image Segmentation

Taherh Hassan Zadeh Koohi, Len Hamey, Kevin Ho-Shon

Department of Computing, Macquarie University, Balaclava Road, North Ryde, Sydney, NSW, 2109, Australia.

tahereh.hassan-zadeh-koohi@hdr.mq.edu.au

Abstract

To improve the FCNN performance for prostate MRI segmentation, we suggest eight different FCNN–based deep 2D network structures for automatic MRI prostate segmentation. Our best 2D network outperforms the state–of–the–art 3D FCNN–based methods for prostate MRI segmentation on publicly available data, without any further post–processing.

Introduction

The purpose of medical image segmentation is using a precise method to find the boundary of a specific organ or tissue, and it is a fundamental step for clinical studies including: diagnosis of disease, monitoring of organs or particular tissues, and, more importantly, treatment planning.

A Fully Convolutional Neural Network (FCNN) is a type of Convolutional Neural Network (CNN) that has been introduced for image segmentation.

we develop new segmentation methods for automatic 2D MRI prostate image segmentation based on U–Net [4] and DenseNet [1] structures. We suggest eight different structures with a particular focus on using various patterns of shortcut connections as well as varying the size of the networks .

Proposed Architecture

We suggest a relatively deep FCNN network structure based on U–Net [4]. The diagram of this architecture is shown in Figure 1.

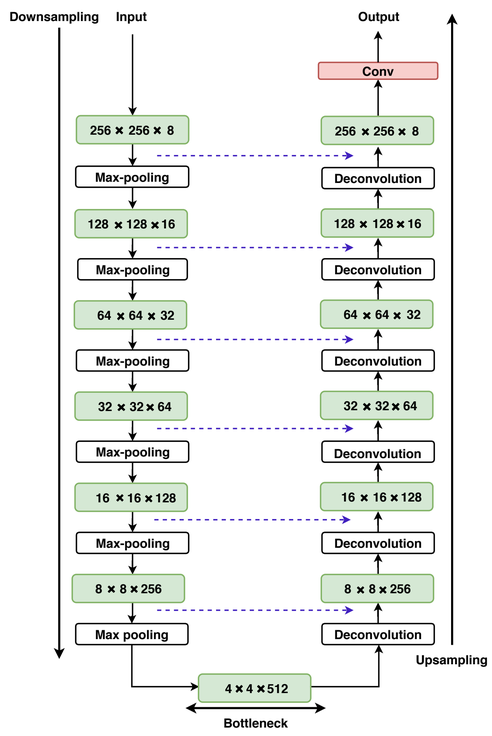

Figure 1: Proposed network architecture for prostate segmentation.

Proposed Blocks

We proposed eight different structures for the blocks. Figure 2, shows the eight block models and they would appear with three layers and each layer includes a convolution layer with kernel size 3×3 follow by a Rectified Linear Unit (ReLU) activation function. To improve the generalisation of the network, batch normalisation and dropout are also employed.

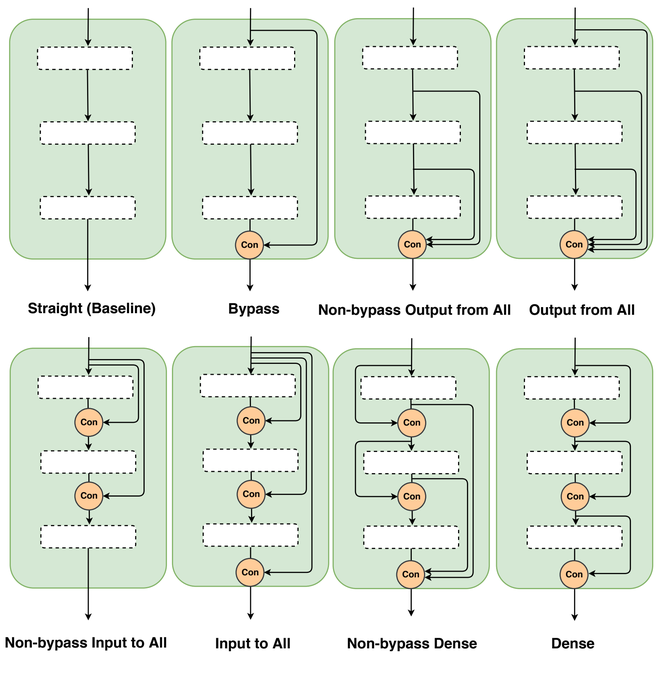

Figure 2: Proposed blocks architecture for prostate segmentation.

Experiments

Dataset and Preprocessing

1. The PROMISE12 challenge dataset [2] is used for studying MRI prostate segmentation. The dataset includes 50 MRI volumes and their corresponding labels for training.
2. For the evaluation of our proposed networks, we apply ten–fold cross–validation on the 50 training volumes.
3. We use the combination of transformations: random rotation within a 10–degree range, horizontal flip, vertical flip, zoom, horizontal and vertical translation, and elastic transformation for augmenting the number of training data to 150000 slices.

Comparison of Proposed Models

Based on the results obtained (see Table 1), using ten–fold cross–validation, the Non–bypass Input to All model is the worst, and Non–bypass Dense model is the best model.

Method	Mean DSC	Median DSC
Mun et al. [3]	0.853	–
Yu et al. [5]	0.869	–
Straight	0.853	0.859
Bypass	0.858	0.863
Non–bypass Output from All	0.849	0.861
Output from All	0.865	0.88
Non–bypass Input to All	0.815	0.82
Input to All	0.819	0.846
Non–bypass Dense	**0.873**	**0.88**
Dense	0.834	0.852

Table 1: Quantitative comparison of proposed models with other models.

Figure 3 and Figure 4 show histograms of the DSC performance across all test images, combining results from all ten folds. It compares the best (Non–bypass Dense) and worst (Non–bypass Input to All) models.

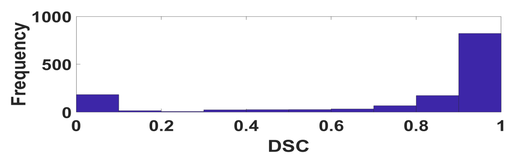

Figure 3: The DSC of the Non–bypass Input to All model based on segmentation of all MRI slices.

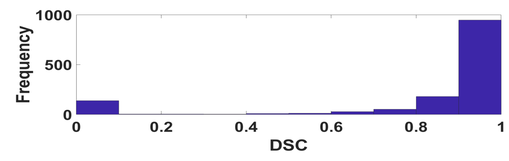

Figure 4: The DSC of the Non–bypass Dense model based on segmentation of all MRI slices.

Also, to show the performance of the best and second-best proposed models for the segmentation of the prostate with the different sizes we provide Figure 5 and Figure 6.

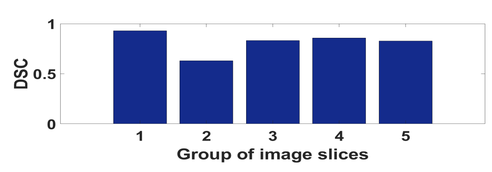

Figure 5: The DSC of the Output from All model based on the size of the prostate.

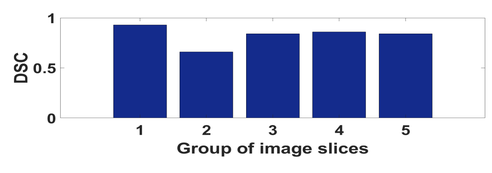

Figure 6: The DSC of the Non-bypass Dense model based on the size of the prostate.

Qualitative Comparison

As a subjective evaluation of the Non–bypass Dense model as the best model, six images selected from the test set of the different folds and the segmentation results are presented in Figure 7 where the red border shows the ground truth and the green border indicates the predicted border.

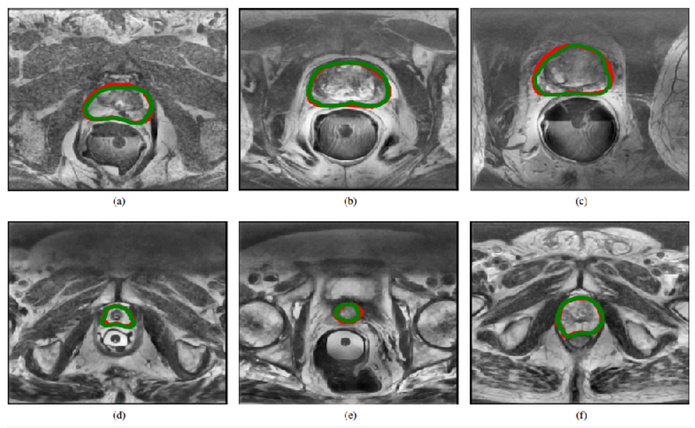

Figure 7: The six sample segmented images using Non-bypass Dense model. The red border is the ground truth and the green border in the predicted border.

Analysing the EndoRectal Coil Effect

To show the effect of ERC (EndoRectal Coil) on the final segmentation results, we evaluate the results of the Output from All and Non–bypass Dense models based on the obtained DSC per volume (see Figure 8 and Figure 9).

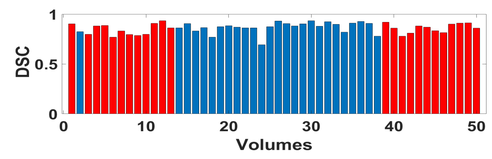

Figure 8: The DSC of the Output from All model based on obtain results per volume. Red bars, ERC–volumes; Blue bars, non–ERC volumes.

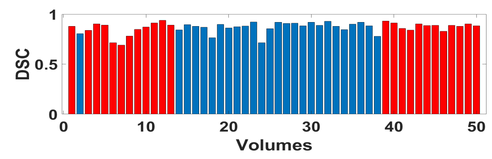

Figure 9: DSC of the Non-bypass Dense model based on obtain results per volume. Red bars, ERC–volumes; Blue bars, non–ERC volumes.

Conclusions

Our proposed Non–bypass Dense model, achieves a new state–of–the–art for FCNN-based prostate segmentation on the PROMISE12 training dataset. The results of our novel structures show the benefits and advantages of reusing the extracted feature maps within and between the blocks, and also the impact of the network structure on the prostate MRI segmentation. Shortcut connections can help their network. However, our results show that using shortcut connections can also decrease the accuracy of the network.

Acknowledgement

This research was undertaken with the assistance of resources and services from the National Computational Infrastructure (NCI), which is supported by the Australian Government.

References

[1] Gao Huang, Zhuang Liu, Laurens Van Der Maaten, and Kilian Q Weinberger. Densely connected convolutional networks. In *CVPR*, volume 1, page 3, 2017.

[2] Geert Litjens, Robert Toth, Wendy van de Ven, Caroline Hoeks, Sjoerd Kerkstra, Bram van Ginneken, Graham Vincent, Gwenael Guillard, Neil Birbeck, Jindang Zhang, et al. Evaluation of prostate segmentation algorithms for mri: the promise12 challenge. *Medical image analysis*, 18(2):359–373, 2014.

[3] Juhyeok Mun, Won-Dong Jang, Deuk Jae Sung, and Chang-Su Kim. Comparison of objective functions in cnn-based prostate magnetic resonance image segmentation. In *Image Processing (ICIP), 2017 IEEE International Conference on*, pages 3859–3863. IEEE, 2017.

[4] Olaf Ronneberger, Philipp Fischer, and Thomas Brox. U-net: Convolutional networks for biomedical image segmentation. In *International Conference on Medical image computing and computer-assisted intervention*, pages 234–241. Springer, 2015.

[5] Lequan Yu, Xin Yang, Hao Chen, Jing Qin, and Pheng-Ann Heng. Volumetric convnets with mixed residual connections for automated prostate segmentation from 3d mr images. In *AAAI*, pages 66–72, 2017.